  Bull. Chem. Soc. Jpn., 65, 2093—2103 (1992)

Equation of State of the Fluid Defined by the Modified Buckingham (exp-6) Potential Derived by Molecular Dynamics Simulations

Yosuke KATAOKA
Department of Chemistry, Faculty of Science, Kyoto University,
Kitashirakawa, Sakyo-ku, Kyoto 606-01
(Received February 24, 1992)

Molecular dynamics simulations have been performed in a wide range of the temperature-density space. The calculated energy and pressure were fitted to obtain the equation of state of the modified Buckingham (exp-6) potential system. This potential function has three parameters; the size, energy, and steepness parameters in the exponential repulsion term. The Helmholtz free energy measured from the ideal gas was expanded in a series of temperature, density, and the steepness parameter. The liquid-gas critical point was examined as a function of the steepness parameter. The liquid–vapor phase boundary was compared with that of the Lennard–Jones fluids. The results reveal how entropy, energy and pressure depend on the steepness parameter.

Equations of state (EOS) of several fluids are derived by computer simulations (Monte Carlo and molecular dynamics method).[1–14] It is important in physical chemistry that the equation of state is known for a system with a given molecular interaction function. The Lennard–Jones (12-6) potential is a typical one, where the equation of state is obtained by computer simulations:[7–13]

$$\phi_{LJ}(r)=4\varepsilon\left[\left(\frac{\sigma}{r}\right)^{12}-\left(\frac{\sigma}{r}\right)^{6}\right].$$

This potential function has only two parameters, i.e., the size parameter σ and the energy parameter ε. For this reason the equation of state is reduced by these parameters and no other parameters remain. Here this potential is too rigid because we can find no more flexibilities to express the complex properties of real fluids other than the two effective potential parameters.

In this paper, we derive the equation of state of the modified Buckingham (exp-6) potential which has three parameters.[15] The third parameter is the steepness parameter of the exponential repulsion term. The first parameter is the molecular separation at the potential minimum, and the second one is the depth of the potential well at the minimum energy.

The potential energy and pressure at many state points calculated by molecular dynamics (MD) simulations for many values of the third parameter will be fitted to obtain the equation of state. The energy and size parameters are used as units to reduce the thermodynamic quantities. The third parameter, however, remains in the equation of state. In this sense, it is much more difficult to determine the equation of state of the system where the interaction function has more than two parameters. On the other hand, systematic studies become possible for such a system. We can change the value of the third parameter to see its effects on many kinds of fluid properties.

Only thermodynamic properties are studied in this paper. It will be shown how these depend on temperature, density and the steepness parameter. Studies on the structure and the dynamic properties will be examined in separate work.

Modified Buckingham Potential

This potential is also called the exp-6 potential. It is written as a function of the molecular distance r as follows:[15]

$$\phi(r)=\frac{\varepsilon}{1-\frac{6}{a}}\left[\frac{6}{a}\exp\left\{a\left(1-\frac{r}{r_m}\right)\right\}-\left(\frac{r_m}{r}\right)^{6}\right],\quad r\geq r_{max},\ (1)$$

$$\phi(r)=\infty,\quad r\leq r_{max}.$$

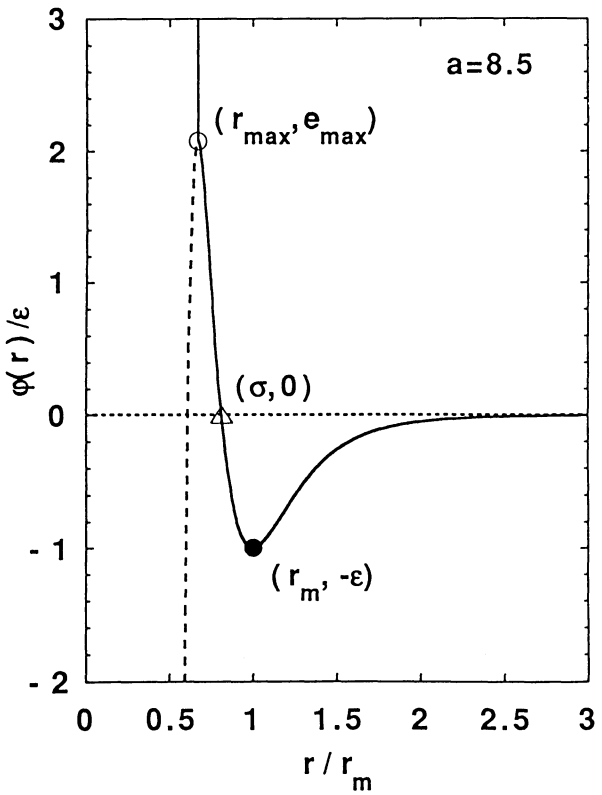

Fig. 1. Modified Buckingham potential as a function of the molecular distance r.

Here r_{max} is the value of r for which $\phi(r)$, as given by the upper relation, has a spurious maximum (Fig. 1). This is a three-parameter potential function in which ε is the depth of the potential at the minimum; r_m is the value of r for the energy minimum; a reflects the steepness of the exponential repulsion. The ratio r_{max}/r_m is given by the smallest root of the equation,

$$\left(\frac{r_{max}}{r_m}\right)^7 \exp\left\{a\left(1-\frac{r_{max}}{r_m}\right)\right\}=1. \quad (2)$$

The diameter σ is defined as the value of r at $\phi(r)=0$. The value of the ratio σ/r_m depends on a in the modified Buckingham (exp-6) potential. For the Lennard-Jones potential (12-6), this ratio is constant: $\sigma/r_m=0.8909$. Figure 2 shows the ratios σ_{max}/r_m and σ/r_m as a function of a. The value of e_{max} is plotted against a in Fig. 3. Hereafter we use the parameter a in the range of $10\leq a\leq 30$. In this case, the spurious maximum is very high as seen from Fig. 3. The ratio σ/r_m has the value: $0.8547\leq\sigma/r_m\leq 0.9323$.

Three cases are compared in Fig. 4: the pair potentials at $a=10$, 14.34 and 30. The case of $a=14.34$ is shown because there the ratio σ/r_m is the same as that of Lennard-Jones potentials. As the potential is normalized by the potential depth ε and the molecular distance r_m at the potential minimum, the potential curve becomes narrower as a increases as shown in Fig. 4.

Molecular Dynamics Simulations

Molecular dynamics calculations were carried out in microcanonical ensemble. The program calculates the temporal evolution of the system using a leapfrog algorithm.[16] The periodic boundary condition is assumed on the cubic cell. The force is cut off at r_{cut} which is half of the MD cell width for the 256-molecule system. The correction term is included by the assumption of the random distribution at, $r>r_{cut}$ in the calculations of energy and pressure. The unit of time τ_0 is defined as by

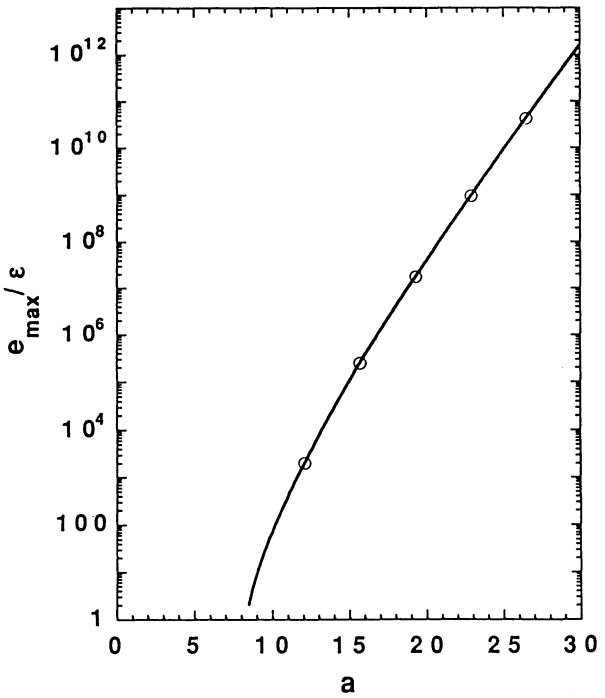

Fig. 3. Plot of e_{max} against a.

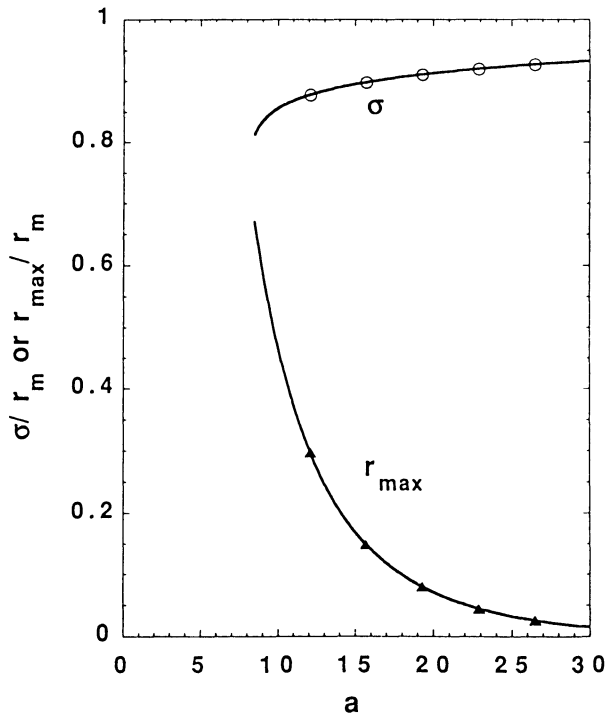

Fig. 2. Ratios r_{max}/r_m and σ/r_m as a function of a.

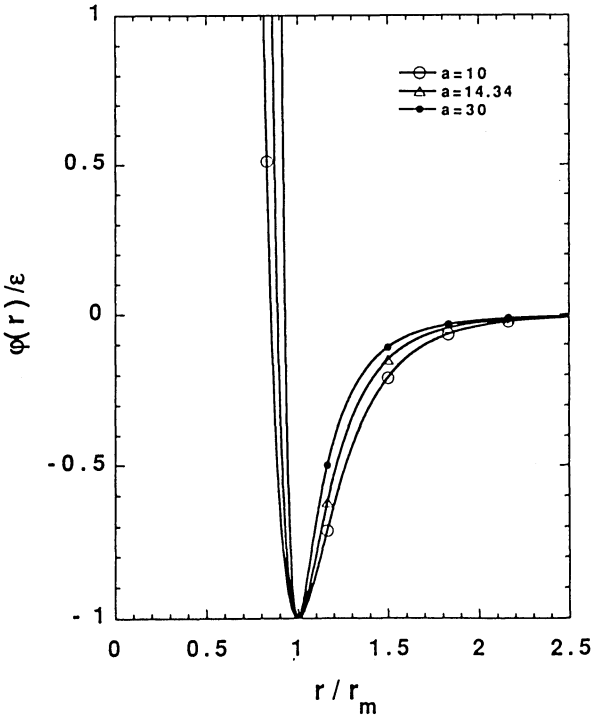

Fig. 4. Pair potential for three values of a.

$$\tau_0 = r_m\sqrt{\frac{m}{\varepsilon}}, \tag{3}$$

where m is the mass. The time step is

$$dt = 0.0045\tau_0, \tag{4}$$

at the typical density and for the value of steepness parameter $a \leq 20$. The time step dt is 0.02 ps in the case of the potential parameters corresponding to liquid CCl_4.[15]

In our run, 5000 steps were spent on aging of the system. After this, a 5000-step run was performed, where the molecular dynamics statistical averages are obtained. This MD run was performed up to 22.5 τ_0, which is 100 ps for the potential parameters corresponding to liquid CCl_4. The cpu time was 0.006 s/step with FACOM VP-2600 at the Kyoto University Data Processing Center and with HITAC S-820/80 at the Computer Center of the Institute for Molecular Science.

Equation of State

Figure 5 is a simulated map of state points. As for the steepness parameter a, the following cases were examined:

$$a = 10, 11.5, 13, 14, 16, 18, 20, 25, 28, 30. \tag{5}$$

The numbers of the states simulated are shown in Fig. 5, where the numbers of the state points with different values of a are summed for simplicity. Full listings of all volumes V, temperatures T, steepness parameters a, energies E, and pressures P are available from the author on request.

The studied volume V has a range:

$$0.76V_0 \leq V \leq 8192V_0. \tag{6}$$

Here V_0 is the volume of a close packed FCC crystal at low temperatures:

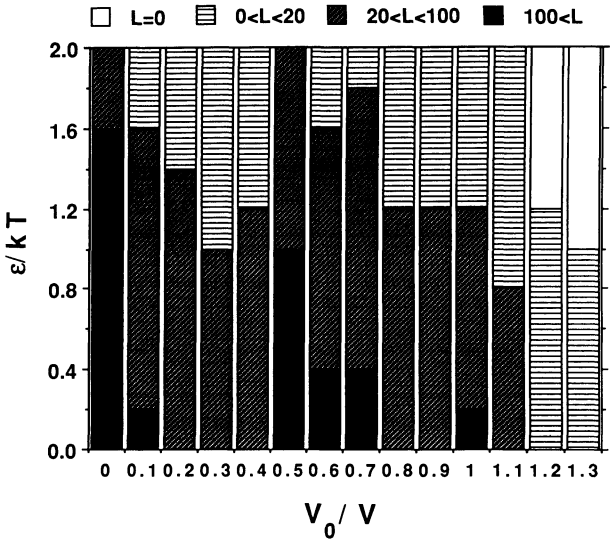

Fig. 5. Map of the simulated states in the (V_0/V, ε/kT) plane. L denotes the number of state.

$$\frac{V_0}{N} = \frac{r_m^3}{\sqrt{2}}, \tag{7}$$

where N is the number of molecules in the system. The state points at a temperature T in the following range (k is the Boltzmann constant):

$$0.5\frac{\varepsilon}{k} < T < 16\frac{\varepsilon}{k} \tag{8}$$

are analyzed although further simulations at lower temperatures are performed to see the liquid-solid transition.

At each volume a random configuration is obtained first and the MD simulation at very high temperatures (about 15 ε/k) is then performed. Then this sample is cooled gradually at constant volume. In this way, a liquid-to-solid transformation is observed at high density ($V \leq V_0$) by monitoring its energy and pressure. When these quantities change to a large extent in a narrow temperature range, it is assigned to a phase transition. The solid state points are omitted by this way in the analysis, where only the fluid states remain.

As for the liquid-gas two phase regions, we assume that the phase separation does not occur in our small (N=256) system simulated for a relatively short time (100 ps for liquid CCl_4). The validity of this assumption will be examined in what follows. All data in the low density region are included to obtain the equation of state of fluid.

Ree's method[11] is used to obtain the equation of state of fluid. By denoting the density N/V and $1/kT$ as ρ and β, respectively, the excess Helmholtz free energy A^e, measured from the ideal gas state, is given as follows:

$$\frac{\beta A^e}{N} = \int_0^\rho \left(\frac{\beta P}{\rho} - 1\right)\frac{1}{\rho}\,d\rho, \tag{9}$$

where the excess internal energy E^e is given by

$$E^e = \left(\frac{\partial \beta A^e}{\partial \beta}\right)_\rho. \tag{10}$$

When the pressure is given as a function of temperature and density,[10] the numerical derivation of the other thermodynamic quantities is not simple. On the other hand, it is easy to obtain thermodynamic quantities from the Helmholtz free energy. For this reason, we assume the following analytic expression for the excess Helmholtz free energy:

$$\frac{\beta A^e}{N} = \sum_p\sum_q\sum_r A_{pqr}\rho_r^p\beta_r^q a_r^r, \tag{11}$$

$$p = 1, 2, 3, 4, 5,$$
$$q = 0, 0.25, 1, 2, 3, \tag{12}$$
$$r = -0.5, 0, 1.5,$$

$$\rho_r = \frac{\rho}{\rho_0},\ \beta_r = \frac{\beta}{\beta_0},\ a_r = \frac{a - a_{00}}{a_0}, \tag{13}$$

$$\rho_0 = \frac{N}{V_0},\ \beta_0 = \frac{1}{\varepsilon},\ a_{00} = 8,\ a_0 = 10. \tag{14}$$

The expansion (11) is a sort of high temperature expan-

sion. Though the exponent q=0.25 may seem odd, this is chosen to express A^e with as a number of terms as small as possible in the trial and error way. Because the equation of state is used in the restricted region (Eq. 8), there are no singularities even with this exponent. The expansion (11) can also be viewed as a density expansion. At the low density limit, only the ρ terms remain. Although the expansion with respect to temperature and density has such a physical meaning, the expansion with respect to a is only a technical way to express the a-dependence of the coefficients in the β- and ρ-expansion. The expansion is performed by means of the dimensionless reduced quantities given by Eqs. 13 and 14.

The coefficients A_{pqr} are obtained by the least-squares fittings. The following quantities are minimized in our case:

$$\sum_i^L\left[\left\{\frac{E_i^e}{N\varepsilon}-\sum_p\sum_q\sum_r qA_{pqr}\rho_{ir}^p\beta_{ir}^{q-1}a_{ir}^r\right\}^2 w_{i,E}+\left\{\left(\frac{\beta_i P_i}{\rho_i}-1\right)\frac{kT_i}{\varepsilon}-\sum_p\sum_q\sum_r pA_{pqr}\rho_{ir}^p\beta_{ir}^{q-1}a_{ir}^r\right\}^2 w_{i,P}\right], \quad (15)$$

$$\rho_{ir}=\frac{\rho_i}{\rho_0},\ \beta_{ir}=\frac{\beta_i}{\beta_0},\ a_{ir}=\frac{a_i-a_{00}}{a_0},\ w_{i,E}=4n_{i\mathrm{MD}},\ w_{i,P}=n_{i\mathrm{MD}}, \quad (16)$$

$$L=7860. \quad (17)$$

Here $n_{i\mathrm{MD}}$ is the MD step number of the i-th MD run. The weights $w_{i,E}$ and $w_{i,P}$ are tentatively chosen as Nicola's case.[10] The number of coefficients A_{pqr} is 75. This is moderate compared with the case of Lennard-Jones fluids where 32 coefficients are used.[10] As there is the third potential parameter in our case, we need more coefficients than the case of the two-parameter, Lennard-Jones potential. The total number of data points 7860 is large enough to determine 75 coefficients. The coefficients A_{prq} are given in Table 1.

Some technical details are described below. The analysis was performed with the statistics package SALS at the Kyoto University Data Processing Center.[17] The coefficients at the low density limit (A_{pqr}, p=1) were determined at first, and then the other coefficients were obtained. It is seen that there are no strong correlations between the basis functions used in the

Table 1. Coefficients A_{pqr} in the Equation of State

p	q	r	A_{pqr}	p	q	r	A_{pqr}
1	0.0	−0.50	−0.6850148	3	2.00	0.0	−6.6081009
1	0.25	−0.50	0.4524021	3	3.00	0.0	12.0017595
1	1.00	−0.50	−0.9978102	3	0.0	1.50	−2.4980745
1	2.00	−0.50	−1.7569237	3	0.25	1.50	6.4317245
1	3.00	−0.50	0.5178725	3	1.00	1.50	−0.2996140
1	0.0	0.0	0.9798958	3	2.00	1.50	−4.2253304
1	0.25	0.0	2.0371027	3	3.00	1.50	1.9814978
1	1.00	0.0	−5.3831902	4	0.0	−0.50	1.3786678
1	2.00	0.0	2.5157204	4	0.25	−0.50	−3.8790855
1	3.00	0.0	−1.3160448	4	1.00	−0.50	1.2802448
1	0.0	1.50	0.1106332	4	2.00	−0.50	15.9196701
1	0.25	1.50	0.0221654	4	3.00	−0.50	−17.1450195
1	1.00	1.50	−0.0927995	4	0.0	0.0	1.8664589
1	2.00	1.50	0.0685976	4	0.25	0.0	−2.6899223
1	3.00	1.50	0.0455256	4	1.00	0.0	10.8094797
2	0.0	−0.50	3.2473965	4	2.00	0.0	6.9019051
2	0.25	−0.50	−7.1216450	4	3.00	0.0	−18.3938751
2	1.00	−0.50	6.3146334	4	0.0	1.50	3.4184790
2	2.00	−0.50	3.9169369	4	0.25	1.50	−8.8453131
2	3.00	−0.50	−5.7430820	4	1.00	1.50	−2.0526648
2	0.0	0.0	−2.6474066	4	2.00	1.50	6.2798786
2	0.25	0.0	6.5439167	4	3.00	1.50	−2.0717278
2	1.00	0.0	−4.2844410	5	0.0	−0.50	1.0566063
2	2.00	0.0	−0.1870927	5	0.25	−0.50	−1.1453161
2	3.00	0.0	−0.6190643	5	1.00	−0.50	1.9671011
2	0.0	1.50	1.1307259	5	2.00	−0.50	−7.9601946
2	0.25	1.50	−2.2454348	5	3.00	−0.50	6.1615953
2	1.00	1.50	0.9304036	5	0.0	0.0	−1.5089417
2	2.00	1.50	0.8111790	5	0.25	0.0	1.0174732
2	3.00	1.50	−0.6701541	5	1.00	0.0	−2.4891043
3	0.0	−0.50	−5.2004805	5	2.00	0.0	−2.3425989
3	0.25	−0.50	9.9220171	5	3.00	0.0	8.2107668
3	1.00	−0.50	−8.3147421	5	0.0	1.50	−1.7408895
3	2.00	−0.50	−10.7043695	5	0.25	1.50	5.0178003
3	3.00	−0.50	16.3647919	5	1.00	1.50	1.4885798
3	0.0	0.0	0.4470198	5	2.00	1.50	−3.0418901
3	0.25	0.0	1.8149662	5	3.00	1.50	0.7206789
3	1.00	0.0	−6.1030884				

expansion Eq. 11.

The relative deviation is obtained as follows:

$$\frac{\left\langle\left[\delta\left(\frac{E^e}{N\varepsilon}\right)\right]^2+\left[\delta\left\{\left(\frac{PV}{NkT}-1\right)\frac{kT}{\varepsilon}\right\}\right]^2\right\rangle^{1/2}}{\left\langle\left(\frac{E^e}{N\varepsilon}\right)^2+\left\{\left(\frac{PV}{NkT}-1\right)\frac{kT}{\varepsilon}\right\}^2\right\rangle^{1/2}}=0.049. \tag{18}$$

The contributions from energy and pressure are shown below:

$$\frac{\left\langle\left[\delta\left(\frac{E^e}{N\varepsilon}\right)\right]^2\right\rangle^{1/2}}{\left\langle\left(\frac{E^e}{N\varepsilon}\right)^2\right\rangle^{1/2}}=0.11, \tag{19}$$

$$\frac{\left\langle\left[\delta\left\{\left(\frac{PV}{NkT}-1\right)\frac{kT}{\varepsilon}\right\}\right]^2\right\rangle^{1/2}}{\left\langle\left\{\left(\frac{PV}{NkT}-1\right)\frac{kT}{\varepsilon}\right\}^2\right\rangle^{1/2}}=0.027. \tag{20}$$

The (V,T) plane is divided into 4 parts as described in Table 2 to see where the deviation comes from. The energy deviation is largest in the low temperature and low density region. On the other hand, the pressure deviation becomes conspicuous at the high temperature and high density region mainly (Table 2).

Figures 6 and 7 show how the least-squares fitting smooths the data. The solid curve represents the EOS, and the circles are the MD result. It is seen that the temperature dependence of pressure and excess internal energy at a given volume is well reproduced.

The volume dependences of pressure and excess internal energy are plotted in Figs. 8 and 9. As the excess internal energy depends only slightly on the density, the shifted excess internal energy $E^e/N\varepsilon+n$, $n=0$ or 1, is plotted in Fig. 8. The curve represents the EOS, and the solid circles show the MD value at the following temperature:

$$1.5\frac{\varepsilon}{k}<T<1.7\frac{\varepsilon}{k}. \tag{21}$$

These are compared with the curve for $T=1.6\,\varepsilon/k$. The open circles correspond to such data for a temperature range:

$$0.95\frac{\varepsilon}{k}<T<1.05\frac{\varepsilon}{k}. \tag{22}$$

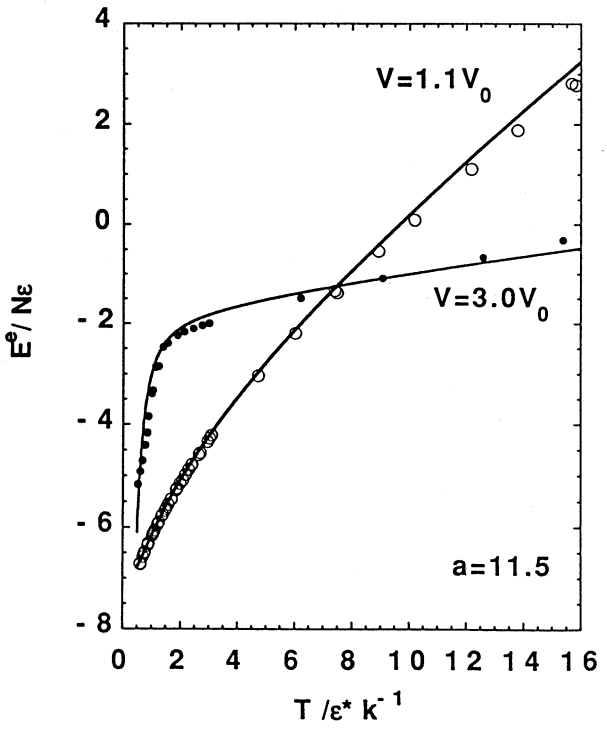

Fig. 6. Examples of fitting of the excess internal energy as a function of temperature at constant volume.

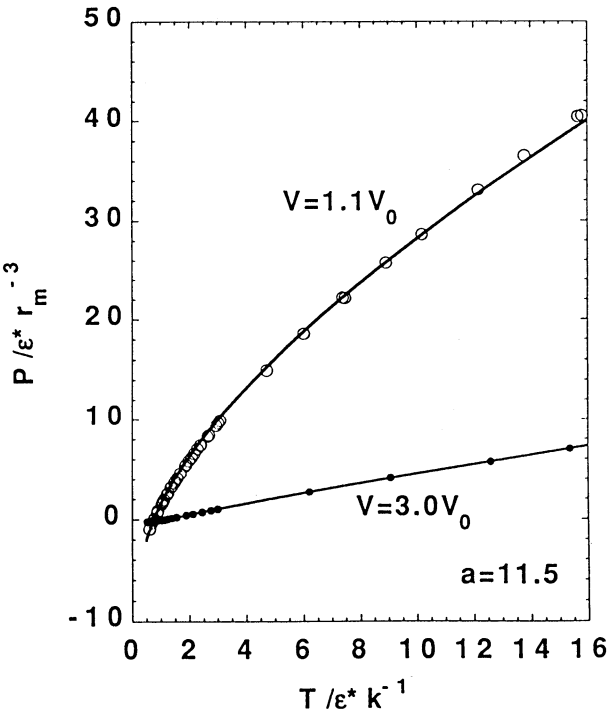

Fig. 7. Examples of fitting of the pressure as a function of temperature at constant volume.

Table 2. Deviations in the Fitting. Ratios of Contributions from Each Part are Shown

	Total deviations		Enegry deviations		Pressure deviations	
	$V>V_0$	$V\leq V_0$	$V>V_0$	$V\leq V_0$	$V>V_0$	$V\leq V_0$
$\varepsilon/kT>1$	0.700	0.005	0.678	0.002	0.022	0.003
$\varepsilon/kT\leq 1$	0.093	0.202	0.034	0.026	0.058	0.176

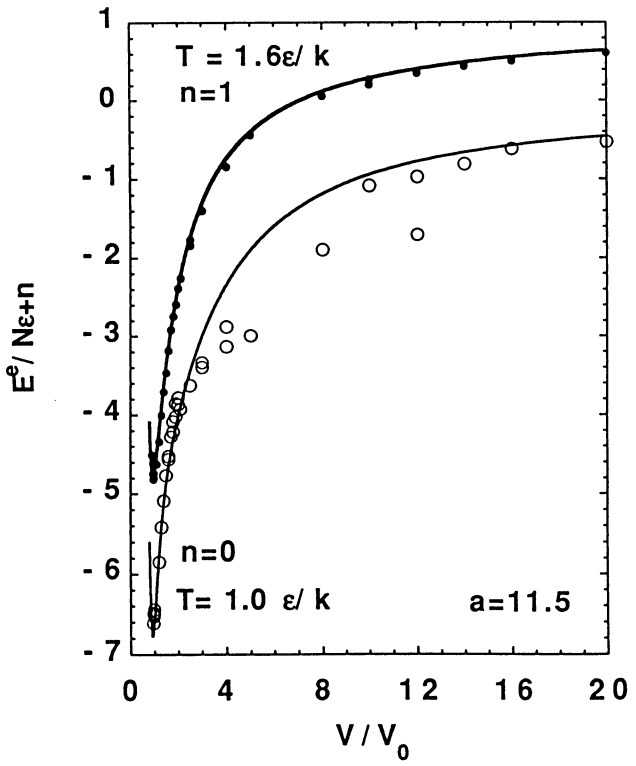

Fig. 8. Volume dependence of the shifted excess internal energy $E^e/N\varepsilon+n$ at constant temperature (n=0 at T=1.0 ε/k, n=1 at T=1.6 ε/k). The curve represents EOS, and the circles are raw MD data (see text and Eqs. 21 and 22).

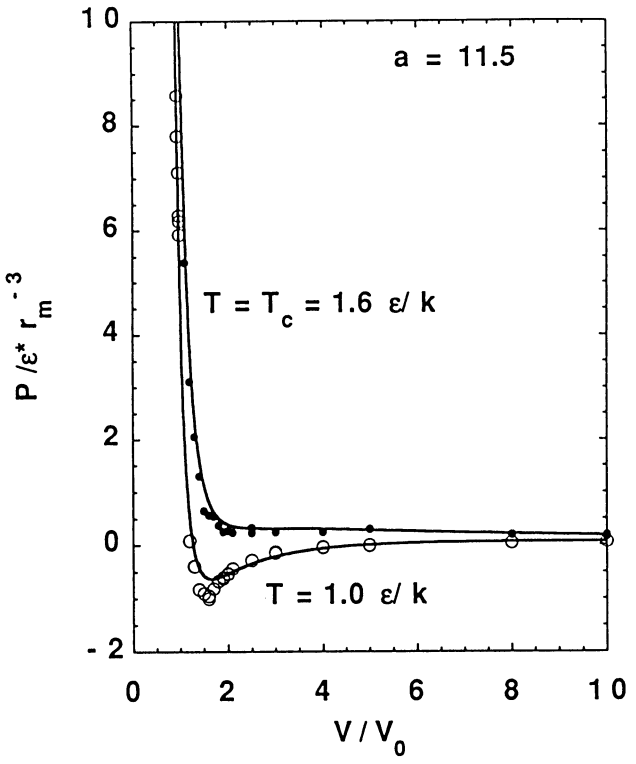

Fig. 9. Volume dependence of the pressure at constant temperature. The curve represents EOS, and the circles are raw MD data (see text and Eqs. 21 and 22).

These data should be compared with the EOS curve at T=1.0 ε/k. The overall feature of MD data is well reproduced by EOS in Figs. 8 and 9. The pressure around $V=3V_0$ at T=1.6 ε/k has a character corresponding to the critical point.

At a lower temperature (T=1.0 ε/k), the excess internal energy curve deviates from the raw data around $V=8V_0$. This means that the liquid and gas phases separate in small parts of the system. It is understood that the phase separation is far from complete by the pressure versus volume data around at T=1.0 ε/k. The metastable and unstable regions are observed in Fig. 9 around $V=2V_0$, at T=1.0 ε/k. Such a situation has been reported for a hard disk system[3] and the Lennard-Jones system.[13]

Thermodynamic Properties and Discussions

The thermodynamic properties thus derived are discussed below. A simple interpretation by the van der Waals approximation is followed by a comparison of some results with those of Lennard-Jones fluids. Several thermodynamical quantities will be plotted to see their dependence on the steepness parameter.

The critical point is discussed first because this is one of the most interesting state points of the fluid. In the next subsection, the liquid-gas phase boundary line is presented. In the third subsection thermodynamic properties are discussed in the (T,P) or (T,V)-plane.

Another discussion will be given in the last subsection, for theoretical interest, on the potential functions which give the same critical temperature and volume.

Critical Point and Comparison with the van der Waals Approximation. In this section we show how the critical point depends on the steepness parameter a in comparison with a simple van der Waals approximation.

The van der Waals EOS is given as follows:[18]

$$P=\frac{NkT}{V-Nb_{\mathrm{vdW}}}-\frac{N^2a_{\mathrm{vdW}}}{V^2}, \tag{23}$$

$$a_{\mathrm{vdW}}=-2\pi\int_{\sigma}^{\infty}\phi(r)r^2\mathrm{d}r, \tag{24}$$

$$b_{\mathrm{vdW}}=\frac{2\pi\sigma^3}{3}. \tag{25}$$

Here the repulsion part is assumed to be a hard sphere with a diameter σ. The attraction part is treated as a perturbation to the hard core system. The free energy of the hard core system is assumed to be the free energy of a perfect gas with volume replaced by a smaller free volume.[18] The critical temperature, volume, and pressure are plotted against the steepness parameter a in Figs. 10, 11, and 12, respectively.

The a-dependences of these quantities are understood qualitatively by van der Waals approximation as follows. The critical point is expressed by the van der Waals constants:

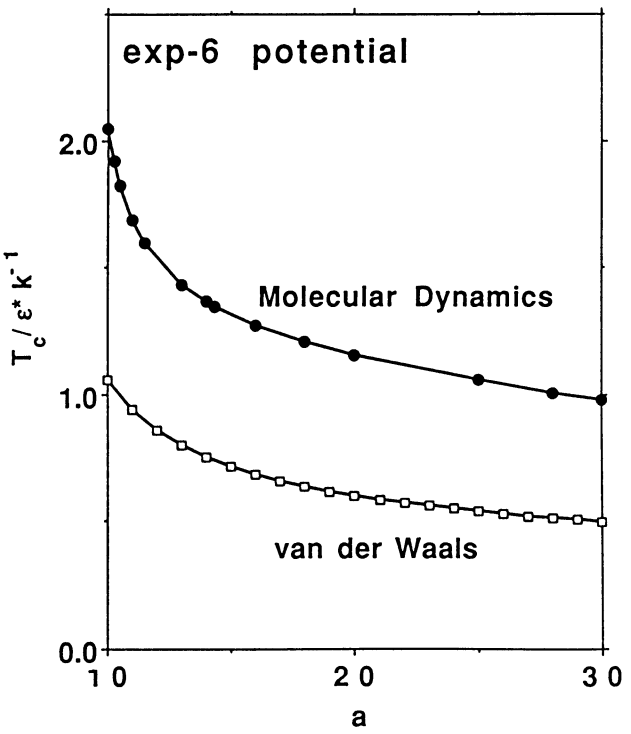

Fig. 10. Critical temperature T_c versus the steepness parameter a. The result with EOS derived by MD is compared with that by the van der Waals approximation.

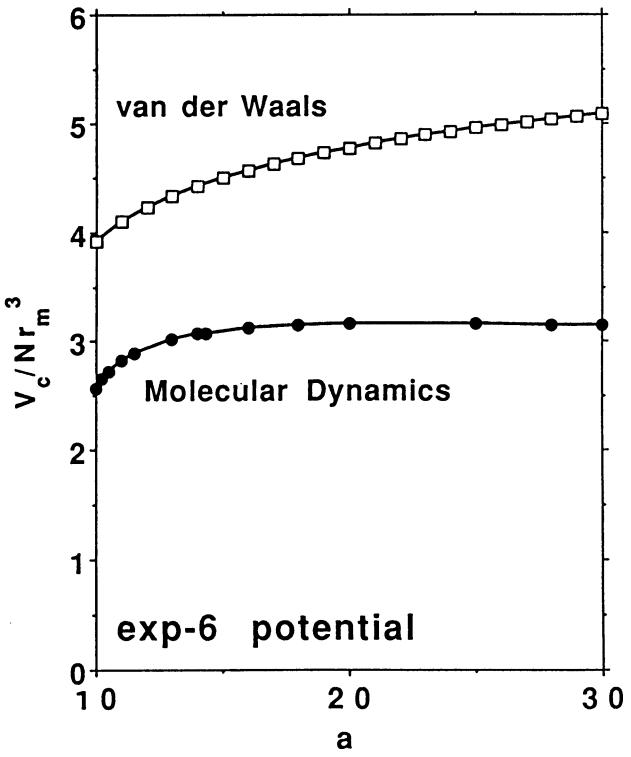

Fig. 11. Critical volume V_c versus the steepness parameter a. The result with EOS derived by MD is compared with that by the van der Waals approximation.

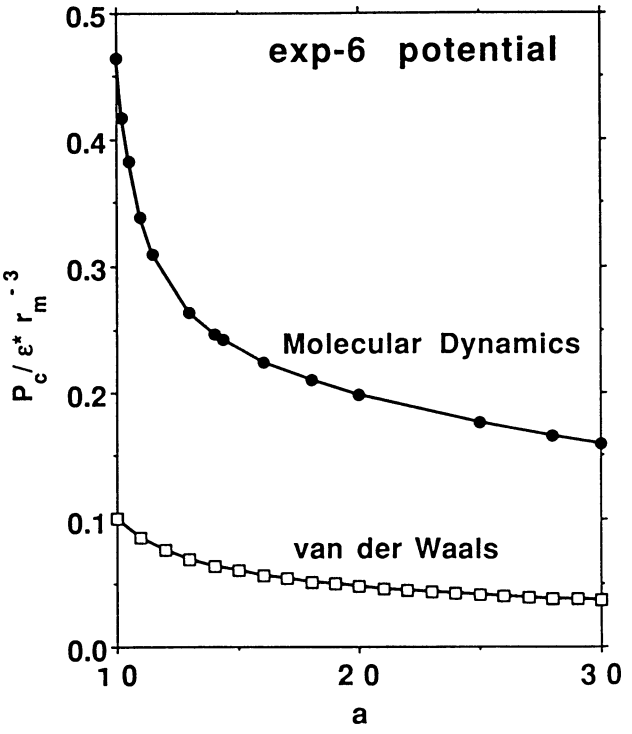

Fig. 12. Critical pressure P_c versus the steepness parameter a. The result with EOS derived by MD is compared with that by the van der Waals approximation.

$$T_c = \frac{8a_{vdW}}{27kb_{vdW}},$$
$$V_c = 3b_{vdW}, \tag{26}$$
$$P_c = \frac{a_{vdW}}{27b_{vdW}^2},$$

The critical temperature is discussed first. The van der Waals constants a_{vdW} and b_{vdW} versus a plots (Fig. 13) shows that the constant a_{vdW} decreases to a greater extent than b_{vdW} with an increase in a. For this reason the critical temperature decreases as a increases in Fig. 10 by the van der Waals approximation. The reason why a_{vdW} decreases with an increase in a is obvious from Fig. 4. Although the absolute value of the critical temperature by this approximation is only about half of the MD result, the relative temperature dependence is well reproduced. We believe that the present approximation gives a simple route to estimate the dependence of the critical temperature on the value of a potential parameter.

It is easy to understand why the critical volume is an increasing function of a by the van der Waals approximation. In this approximation the core size is defined by σ which increases as a increases (Fig. 2). We see that this way of understanding is correct qualitatively by the comparison the MD result with that of the van der Waals approximation in Fig. 11.

The estimated critical pressure by the van der Waals approximation is worst compared with other critical

quantities as shown in Fig. 12. The critical pressure is most difficult to estimate in an approximation.

The compressibility factor at the critical point is shown in Fig. 14 as a function of a. The van der Waals approximation is too crude to give a-dependence of the compressibillty factor at the critical point. The MD result shows that the factor decreases as a increases. The value is larger than that of Lennard-Jones fluids (0.30—0.33).[10,13] In order to see this difference critical quantities are compared in Table 3, where a is 14.34 because at this value σ has the same value as in the Lennard-Jones potential. It is seen that a large value of the critical pressure is the main reason for a large compressibility factor in the exp-6 potential.

Although the compressibility factor is an indicator to specify real fluids, we believe EOS should be compared with the observed data in a wide range. In this sense, we hope the present EOS is used in the analysis of real fluids. The FORTRAN program to calculate the thermodynamic quantity from the EOS is available from the author on request.

Liquid-Gas Phase Boundary. In Fig. 15 the liquid-gas phase boundary is displayed. It is seen that the

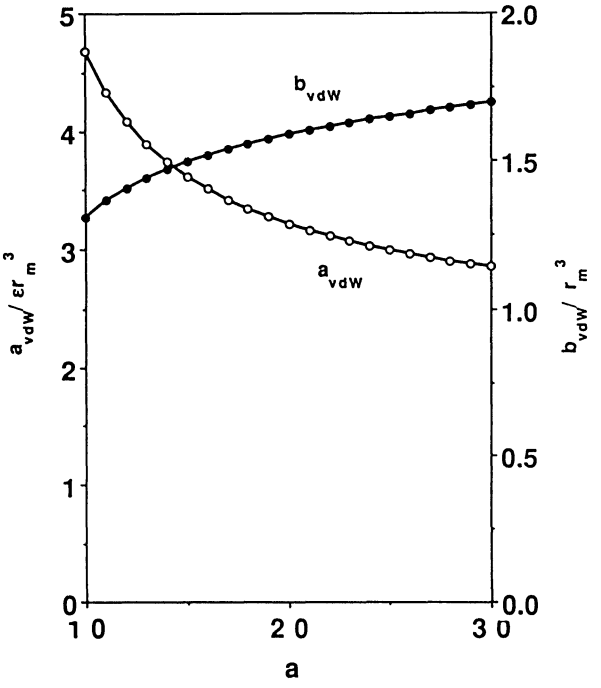

Fig. 13. Van der Waals constants a_{vdW} and b_{vdW} as a function of a.

Table 3. Critical Constants of the Modified Buckingham (exp-6) and Lennard-Jones Potential Fluids

	exp-6	Lennard-Jones	
	a=14.34	Nicolas et al.[10]	Adachi et al.[13]
$P_c/\varepsilon\sigma^{-3}$	0.17	0.14	0.12
$V_c/N\sigma^3$	3.08	2.86	3.52
$T_c/\varepsilon k^{-1}$	1.35	1.35	1.27
$P_cV_c/(NkT_c)$	0.39	0.30	0.33

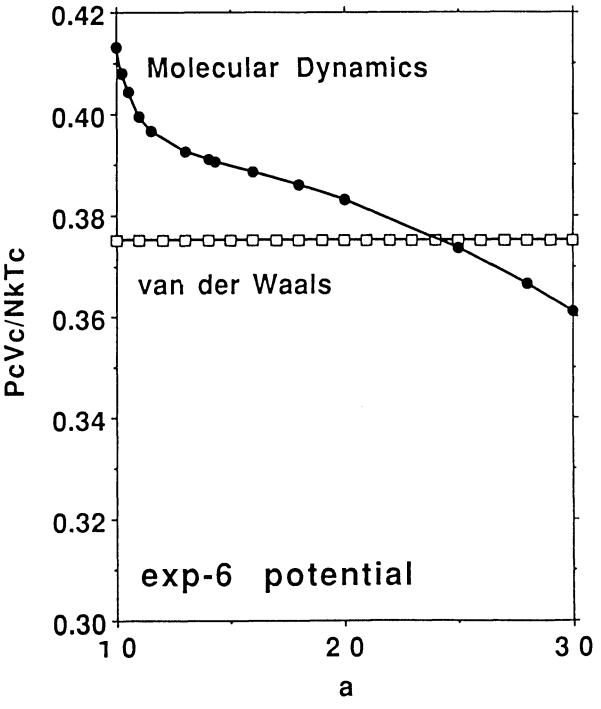

Fig. 14. Compressibility factor PV/NkT at the critical point versus the steepness parameter a. The result with EOS derived by MD is compared with that by the van der Waals approximation.

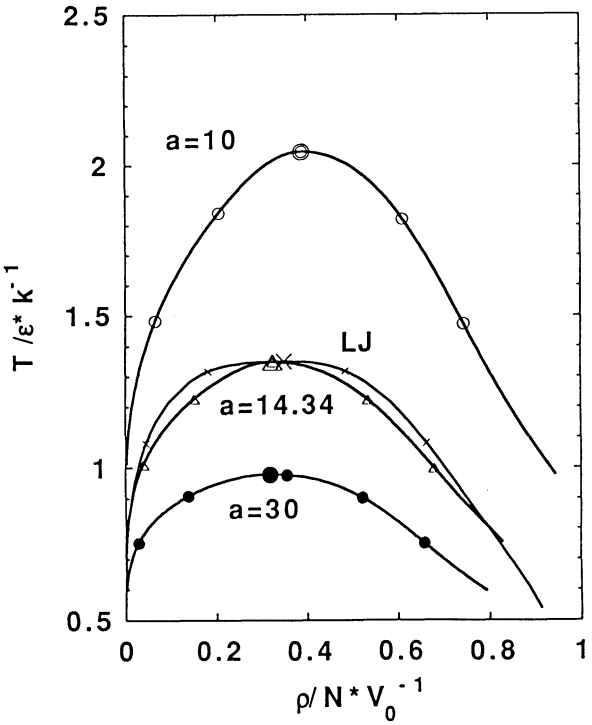

Fig. 15. Liquid-gas phase boundary for a=10, 14.34, and 30. The large mark represents the critical point. The Lennard-Jones case is also shown.

phase boundary moves to a large extent as a changes. The case of a=14.34 is compared with that of Lennard-Jones fluids. The phase boundary at a=14.34 almost coincides with that of Lennard-Jones fluids. This is in contrast with the large (ca. 20%) difference in the compressibility factor at the critical point. The critical point is shown by the large mark in Fig. 15, where we can see how the critical point depends on the steepness parameter a in the (ρ,T)-plane.

Dependence of Thermodynamic Properties on the Steepness Parameter. We are going to see how the P-V-T relation depends on the steepness parameter. The reduced forms of P-V-T curves at the critical temperature for three values of a are close to each other (not shown in figure). For details, the reduced volumes at the critical temperature divided by that of the van der Waals EOS are plotted against the reduced pressure in Fig. 16. The about 10% difference is observed in the three curves of the modified Buckingham potential fluids. The reduced volume of the Lennard-Jones fluids is larger than that of the exp-6 cases in almost all the region in Fig. 16. In this figure is plotted a curve of Lennard-Jones fluids outside the region where those of the exp-6 fluids are found except around the P=P_c. This means that a difference in the functional form of the pair potential is significant for the P-V-T relation.

Now the second derivatives of the free energy are discussed. The isothermal compressibility, thermal expansion coefficient and heat capacity at constant

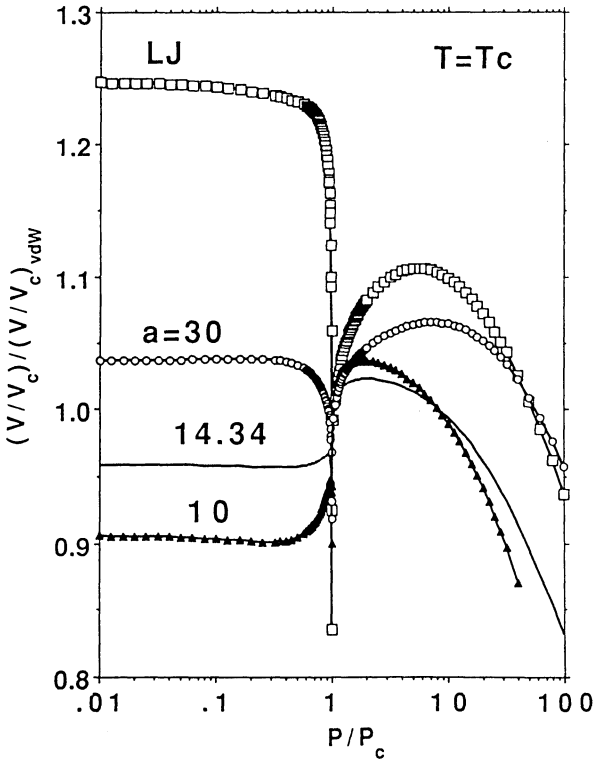

Fig. 16. Reduced volume $(V/V_c)/(V/V_c)_{vdW}$ versus the reduced pressure P/P_c at the critical temperature for a=10, 14.34, and 30.

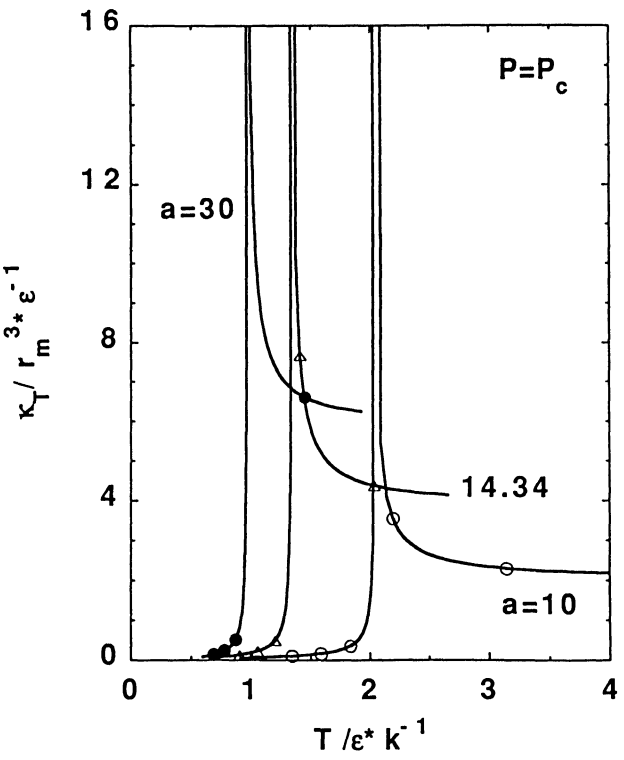

Fig. 17. Isothermal compressibility k_T versus temperature T plot at the critical pressure for a=10, 14.34, and 30.

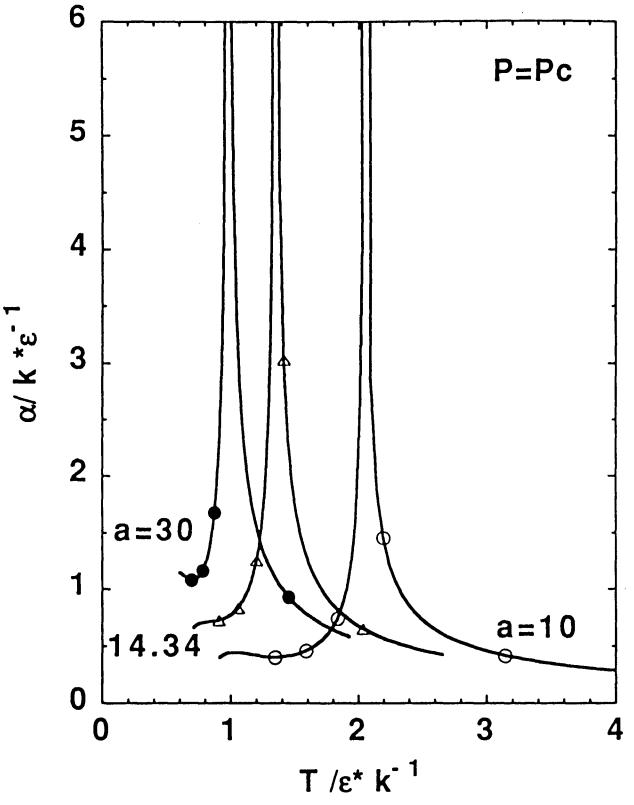

Fig. 18. Thermal expansion coefficient α versus temperature T at the critical pressure for a=10, 14.34, and 30.

volume are shown at the critical pressure in Figs. 17, 18, and 19, respectively. Among the three figures the a dependence of the heat capacity at constant volume is most significant. These quantities are plotted against temperature also at $P=0.1P_c$ and $2P_c$, though these are not shown in figures. These results can be summarized as the follows. As for the isothermal compressibility factor and the thermal expansion coefficient, the volume is more sensitive to the change of pressure or temperature for larger values of the steepness parameter a, as expected by the pair potential shown in Fig. 4.

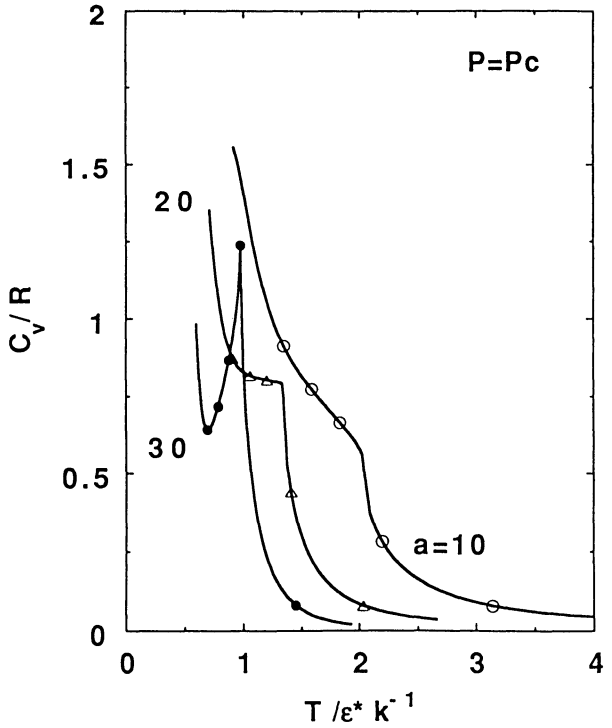

Fig. 19. Heat capacity at constant volume C_v versus temperature T at the critical pressure for a=10, 14.34, and 30. R is the gas constant Nk.

The temperature dependence of the extensive quantities at the constant volume condition is easier to understand than that at the constant pressure condition. In Figs. 20 and 21, the excess entropy and the excess internal energy are plotted against temperature at the critical volume. Similar plots are obtained at $V=0.4V_c$ and $0.7V_c$ (not shown). The excess entropy is lower for larger values of the steepness parameter and concomitantly the excess internal energy is higher as seen in Figs. 20 and 21. It is not difficult to understand these a-dependences by the width of the pair potential well in Fig. 4. As the excess internal energy is an average of the pair potential, the potential function with a wider range of the attractive part gives a lower energy as in Fig. 21. The excess entropy (Fig. 20) is interesting, when it is seen as a function of a. This figure shows that the order is established relatively more by the narrower potential well.

Potential Functions Which Give the Same Critical Temperature and Volume. The three potential functions which give the same critical temperature and volume are compared in Fig. 22. Here $\varepsilon(a)$ and $V_0(a)$ are regarded as functions of the steepness parameter a,

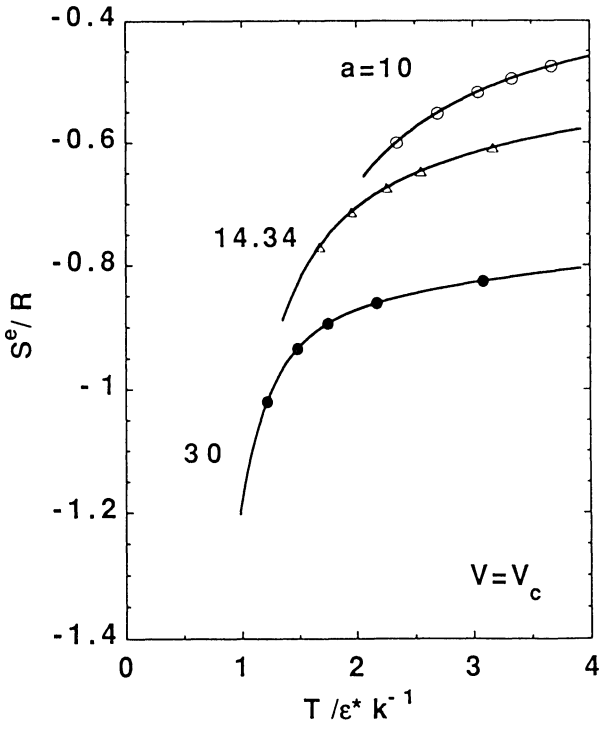

Fig. 20. The excess entropy S^e versus temperature T at the critical volume for a=10, 14.34, and 30.

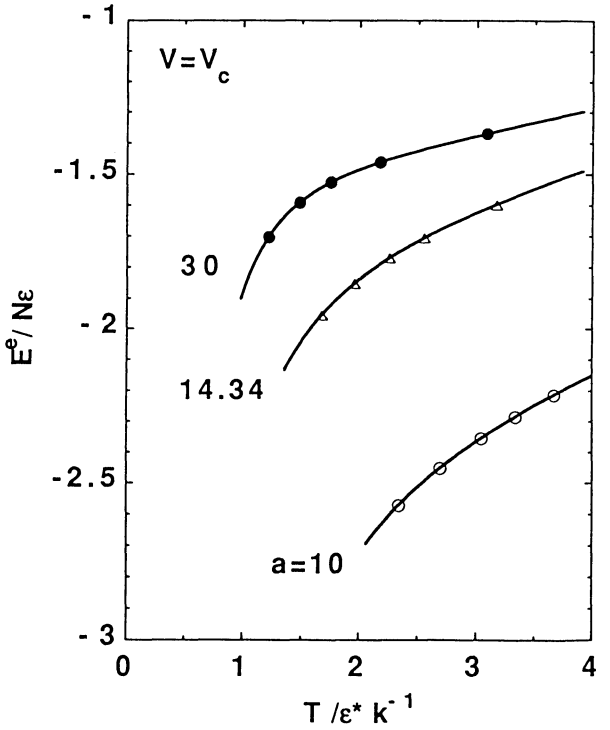

Fig. 21. Excess internal energy E^e versus temperature T at the critical volume for a=10, 14.34, and 30.

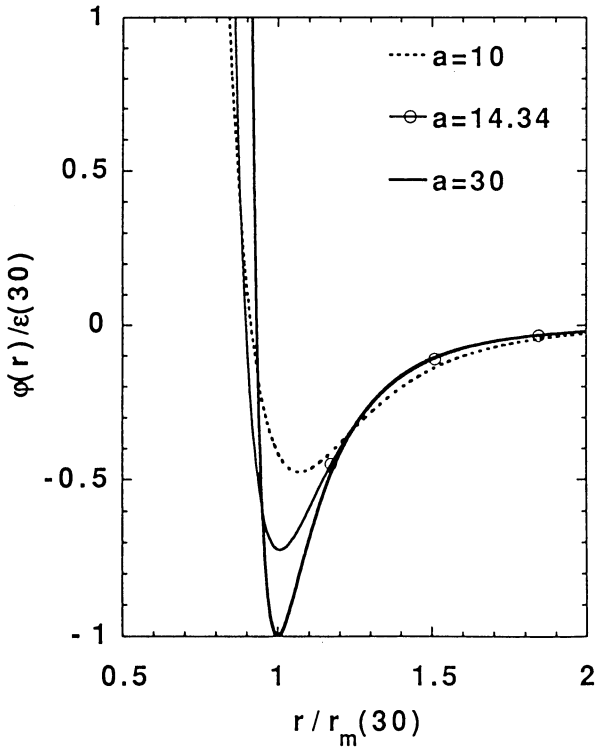

Fig. 22. Pair potentials which give the same critical temperature and volume are compared for a=10, 14.34, and 30.

because we can choose suitable values as ε and V_0 (or r_m) for each value of a. Figure 22 is obtained by the equations:

$$T_c=\frac{2.05\varepsilon(10)}{k}=\frac{1.35\varepsilon(14.34)}{k}=\frac{0.98\varepsilon(30)}{k}, \tag{27}$$

$$V_c=2.57V_0(10)=3.08V_0(14.34)=3.14V_0(30). \tag{28}$$

The critical pressures are related with ε and V_0 as follows:

$$P_c(10)=\frac{0.329\varepsilon(10)}{V_0},$$
$$P_c(14.34)=\frac{0.171\varepsilon(14.34)}{V_0}, \tag{29}$$
$$P_c(30)=\frac{0.112\varepsilon(30)}{V_0}.$$

By combining Eqs. 27—29 we obtain

$$P_c(10)=1.14P_c(30),$$
$$P_c(14.34)=1.08P_c(30). \tag{30}$$

It is interesting that the ratio of the two critical pressures is only 1.14 (Eq. 30) in contrast to a large difference in the pair potentials shown in Fig. 22.

The author would like to thank Professor Nobuhiro Go for valuable discussions. This work was supported in part by Grants-in-Aid for Scientific Research Nos. 01540398, 02245209, and 03231211 from the Ministry of Education, Science and Culture, and in part by the Japan Society for the Promotion of Science and Japan/U.S. Research Cooperation. The author thanks the Computer Center of the Institute for Molecular Science for the use of HITAC M-680H and S-820/80 computers. The computation was also done with FACOM VP-2600 at the Kyoto University Data Processing Center, and Stardent TITAN in our laboratory.

References

1) N. Metropolis, A. W. Rosenbluth, M. N. Rosenbluth, A. H. Teller, and E. Teller, *J. Chem. Phys.*, **21**, 1087 (1953).
2) B. J. Alder and T. E. Wainwright, *J. Chem. Phys.*, **27**, 1208 (1957).
3) B. J. Alder and T. E. Wainwright, *Phys. Rev.*, **127**, 359 (1962).
4) H. N. V. Temperley, J. S. Rowlinson, and G. S. Rushbrooke, "Physics of Simple Liquids," North Holland, Amsterdam (1968).
5) W. G. Hoover, M. Ross, K. W. Johnson, D. Henderson, J. A. Barker, and B. C. Brown, *J. Chem. Phys.*, **52**, 4931 (1970).
6) W. G. Hoover, S. G. Gray, and K. W. Johnson, *J. Chem. Phys.*, **55**, 1128 (1970).
7) J. P. Hansen, *Phys. Rev. A*, **2**, 221 (1970).
8) I. R. McDonald and K. Singer, *Mol. Phys.*, **23**, 29 (1972).
9) D. J. Adams, *Mol. Phys.*, **37**, 211 (1979).
10) J. J. Nicolas, K. E. Gubbins, W. B. Streett, and D. J. Tildesley, *Mol. Phys.*, **37**, 1429 (1979).
11) F. H. Ree, *J. Chem. Phys.*, **73**, 5401 (1980).
12) J. Sys and A. Malijevsky, *Collect. Czech. Chem. Commun.*, **45**, 1155 (1980).
13) Y. Adachi, I. Fijihara, M. Takamiya, and K. Nakanishi, *Fluid Phase Equilib.*, **39**, 1 (1988).
14) Y. Kataoka, *J. Chem. Phys.*, **87**, 589 (1987).
15) J. O. Hirschfelder, C. F. Curtiss, and R. B. Bird, "Molecular Theory of Gases and Liquids," John Wiley & Sons, New York (1954).
16) M. P. Allen and D. J. Tildesley, "Computer Simulation of Liquids," Oxford Univ. Press, Oxford (1987).
17) T. Nakagawa and Y. Oyanagi, "Recent Developments in Statistical Interface and Data Analysis," ed by K. Matusita, North Holland, Amsterdam (1980), p. 221.
18) See for example, J. A. Barker and D. Henderson, *Rev. Mod. Phys.*, **48**, 587 (1976).